

Supplementary Information

3-D Electrochemical Impedance Spectroscopy Mapping of Arteries to Detect Metabolically Active but Angiographically Invisible Atherosclerotic Lesions

René R. Sevag Packard* ^{1,2,3}, Yuan Luo* ⁴, Parinaz Abiri ^{1,5}, Nelson Jen ^{1,2}, Olcay Aksoy ^{1,2}, William M. Suh ^{1,2}, Yu-Chong Tai ⁴, Tzung K. Hsiai ^{1,2,3,5}

¹ Division of Cardiology, Department of Medicine, David Geffen School of Medicine, University of California, Los Angeles, California

² Ronald Reagan UCLA Medical Center, Los Angeles, California

³ Veterans Affairs West Los Angeles Medical Center, Los Angeles, California

⁴ Electrical and Mechanical Engineering, California Institute of Technology, Pasadena, California

⁵ Department of Bioengineering, Henry Samueli School of Engineering and Applied Sciences, University of California, Los Angeles, California

* Equal contribution

I. Bode diagrams of Z_{CPE} obtained from fitting using the two circuit models

As shown in the main text:

$$Z_{CPE} = \frac{1}{Y(j\omega)^a}$$

where Y denotes the empirical admittance value, and a is a constant between 0 and 1, ω is the angular frequency and $j = \sqrt{-1}$. Fitting from the two circuit models (Fig. 3g & h) yields two sets of Y and a : $321 \text{ nS} \cdot \text{s}^a / 0.691$ and $248 \text{ nS} \cdot \text{s}^a / 0.659$, for balloon deflation and inflation, respectively. The Bode diagrams are shown in Fig. S1. Their behavior is similar to that of a typical capacitance, i.e. being linear in magnitude and constant in phase.

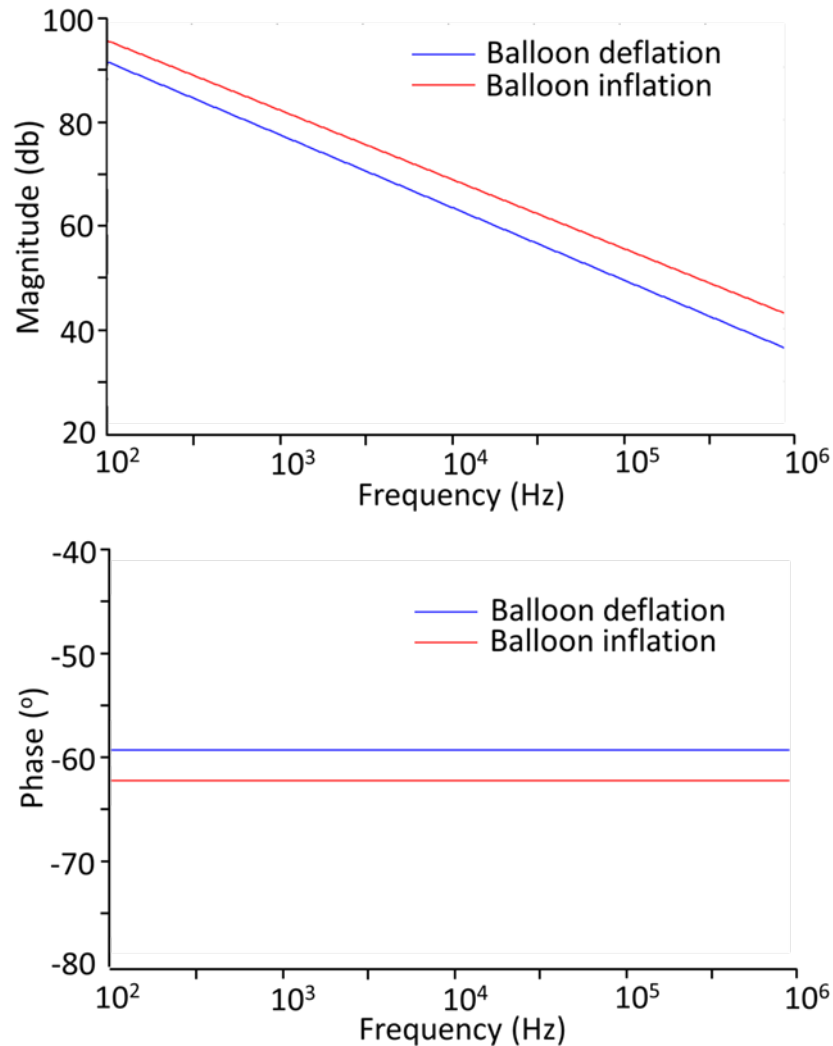


Figure S1. Bode diagrams (magnitude / phase) illustrating the behavior of the constant phase element under balloon deflation and inflation.

II. Discussion on the circuit modeling fitting

For each tissue type (blood, aorta, plaque, perivascular fat), the total impedance can be written based on the circuit model in Fig. 3g in the main text as:

$$Z = A - B \cdot j \quad (1)$$

$$A = \frac{\omega^2 C^2 R_1 R_2 (R_1 + R_2) + R_1}{1 + \omega^2 C^2 (R_1 + R_2)^2} \quad (2)$$

$$B = \frac{\omega C R_2^2}{1 + \omega^2 C^2 (R_1 + R_2)^2} \quad (3)$$

where ω denotes the angular frequency, $j = \sqrt{-1}$, R_1, R_2 and C represent the two resistances and capacitance value from the circuit model.

To demonstrate that the fitting results of all the resistance and capacitance (shown below in Table I) from different tissues are reasonable, we present a physical model that uses the intrinsic electrical properties and geometric factors of each tissue to obtain their impedance value, which will then be compared with the Z shown above.

First, the cross-sectional schematics showing the relative position of electrodes and different tissues under either balloon inflation or deflation are depicted in Fig. S2. The condition shown in Fig. S2a corresponds to the circuit model presented in Fig. 3g in the main text and will be utilized for validating the parameters for blood. The scenario in Fig. S2b (modeled as Fig. 3h in the main text) will be considered for aorta wall, plaque, and perivascular fat as the dimension of blood is difficult to estimate when the balloon is inflated.

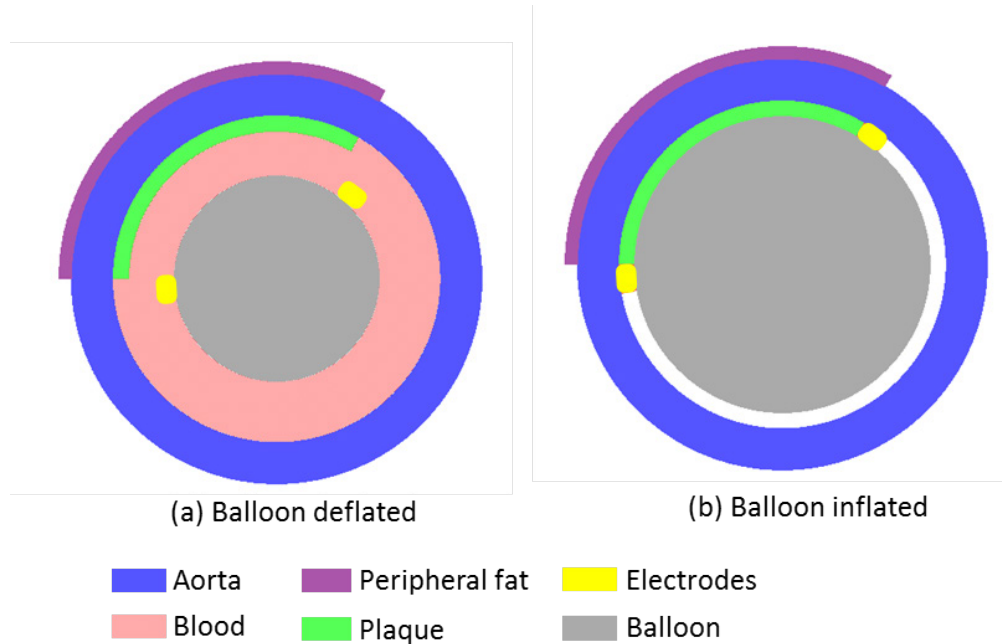


Figure S2. Cross-sectional perspective of the *in vivo* electrode positioning with respect to the aortic cross-section under interrogation under balloon (a) deflated and (b) inflated conditions.

For plaque and perivascular fat, we consider a simple impedance model as shown in Fig. S3a. The impedance of the tissue can be written as [1]:

$$Z' = \frac{1}{j\omega\varepsilon^*G} \quad (4)$$

where ε^* represents the complex permittivity:

$$\varepsilon^* = \varepsilon\varepsilon_0 - \frac{j\sigma}{\omega} \quad (5)$$

where σ , ε denotes the conductivity and relative permittivity of the tissue, $\varepsilon_0 = 8.85\text{e-}12$ F/m the vacuum permittivity, and $G = ad/l$ the geometric factor. For plaque and perivascular fat, we consider the scenario in Fig. S3a, and based on the histology image in Fig.3 from main text we estimate $l = 2\pi r/3$. Note that the electrode pair shown in Fig. S3 is separated by 1/3 of the circumference due to our design (see Fig. 1 in main text). For blood and the aorta wall (as a complete circular object), we consider the scenario shown in Fig. S3b where 1/3 of the tissue is in parallel with the remaining 2/3, therefore yielding an effective $l = 4\pi r/9$.

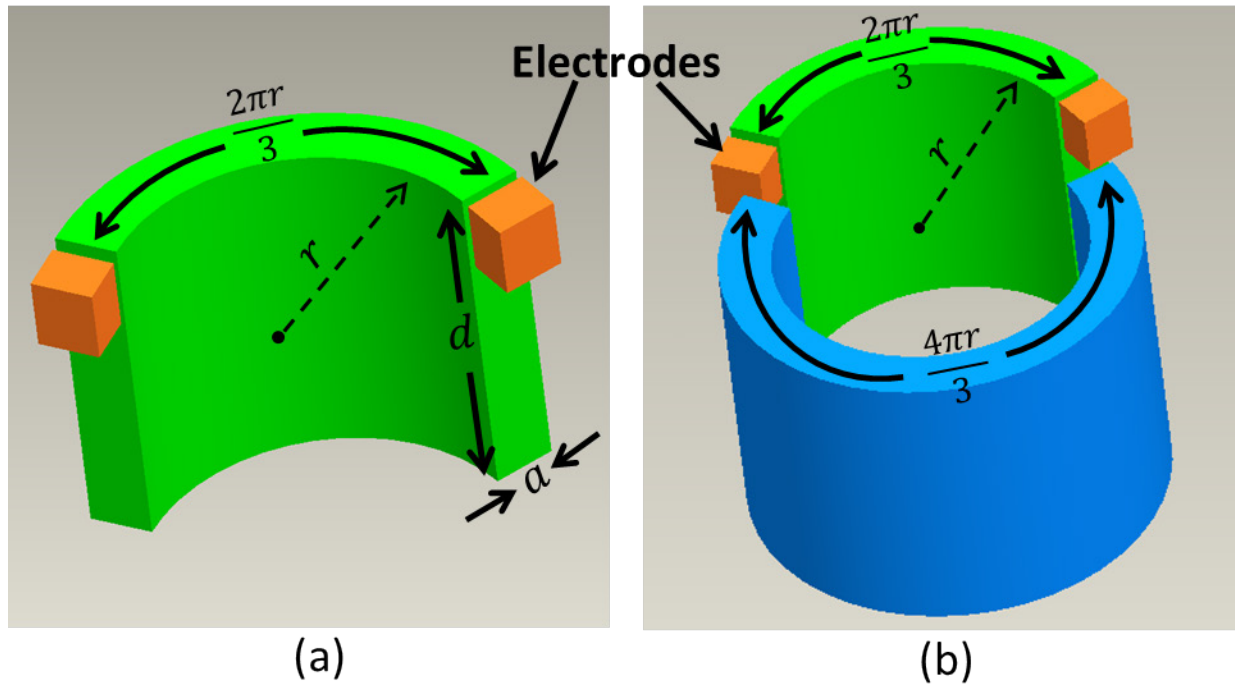


Figure S3. 3D rendering of tissue model impedance calculation parameters of the electrodes on the sensor (a) and the sensor in contact with the aorta (b).

From equation (4) and (5) we can obtain the impedance value of each tissue merely based on their intrinsic electrical properties and geometrical variables:

$$Z' = A' - B' \cdot j \quad (6)$$

$$A' = \frac{\sigma l}{ad(\sigma^2 + \omega^2(\epsilon\epsilon_0)^2)} \quad (7)$$

$$B' = \frac{\omega\epsilon\epsilon_0 l}{ad(\sigma^2 + \omega^2(\epsilon\epsilon_0)^2)} \quad (8)$$

Z will be calculated using the fitting results, and Z' is achieved through the electrical properties of different tissues and geometric variables estimated from the histology image (as shown in Fig. 3 in the main text). We chose $\omega=10$ kHz for all of our calculation. Table S1 shows the achieved resistance and capacitance values for each of the tissues obtained from fitting. Table S2 lists all the parameters used in the calculation. Table S3 shows the comparison between the results obtained from the circuit model and the results from the physical model (A, B, A', B'). As seen, results from the two sets of calculation are all within an order of magnitude of each other. The source of discrepancy could rise from: a) the irregularity of the actual tissue geometry as compared to the simple geometry used in the calculation; b) there is a relatively wide range of reported electrical property values of individual tissues, e.g. the conductivity of fat varies around 3-5 fold in the published literature [2, 3, 4]. In conclusion, the presented circuit model can reasonably describe the actual electrical behavior of the multiple existing tissues.

Table S1. Fitting results from the circuit model presented in the main text

	Blood* (From Fig.3g)	Blood (From Fig.3h)	Aorta	Plaque	Perivascular fat
R_1 (ohm)	0.1	50	0.7	1.25e3	258
R_2 (ohm)	1682	2.42e4	1.79e4	2.95e4	8.49e4
C (F)	138e-12	29.7e-12	0.35e-12	10.0e-12	82.5e-12

*Only the fitting results for blood obtained from model circuit in Fig. 3g from the main text is used for the calculation.

Table S2. Electrical properties and geometrical valuables of different tissue used in the calculation

	Blood	Aorta	Plaque [†]	Perivascular fat [†]
a (mm)	1	0.6	0.2	0.1
d (mm)	3	3	3	3
l (mm)	$4\pi \times 1.2/9$	$4\pi \times 1.9/9$	$2\pi \times 1.6/3$	$2\pi \times 2.2/3$
σ^* (S/m)	0.70	0.31	0.043	0.043
ϵ^*	5250	7690	912	912

* Conductivity and relative permittivity values are obtained from [4].

† Conductivity and relative permittivity of fat are used.

Table S3. Comparison of impedance values

	<i>A</i>	<i>B</i>	<i>A'</i>	<i>B'</i>
Blood	1.6820e+3	3.9042	7.9786e+2	0.5098
Aorta	1.7940e+4	1.1232	4.7088e+3	9.8465
Plaque	2.9500e+4	87.3246	1.2988e+5	234.529
Peripheral fat	8.4470e+4	5.9174e+3	3.5718e+5	6.4544e+2

References

1. Sun T, Catia B, Hywel M. Single-colloidal particle impedance spectroscopy: Complete equivalent circuit analysis of polyelectrolyte microcapsules. *Langmuir*. 2009; 26: 3821-8.
2. Awada K, Jackson DR, Baumann SB, Williams JT, Wilton DR, Fink PW, Prasky BR. Effect of conductivity uncertainties and modeling errors on EEG source localization using a 2-D model. *IEEE Transactions on Biomedical Engineering*. 1998; 45: 1135-45.
3. Gabriel C, Gabriel S, Corthout E. The dielectric properties of biological tissues: I. Literature survey. *Physics in Medicine and Biology*. 1996; 41: p. 2231.
4. Hasgall PA, Di Gennaro F, Baumgartner C, Neufeld E, Gosselin MC, Payne D, Klingeböck A, Kuster N. "IT'IS Database for thermal and electromagnetic parameters of biological tissues," Version 3.0, September 1st, 2015. DOI: 10.13099/VIP21000-03-0.